NUMERICAL MODEL OF A BURNING WOOD CYLINDER

Fernando de Souza Costa
Laboratório Associado de Combustão e Propulsão, INPE
Rodovia Presidente Dutra, km 40, Cachoeira Paulista, SP, 12630-000
e-mail: fernando@lcp.inpe.br

André de Castro
Laboratório Associado de Combustão e Propulsão, INPE
Rodovia Presidente Dutra, km 40, Cachoeira Paulista, SP, 12630-000
e-mail: andre@lcp.inpe.br, andredecastro@gmail.com

Abstract. *The burning of wood presents several phases: pre-heating, water vaporization of water, pyrolysis, ignition, flaming, extinction of the flame, smoldering, and final extinction. It is a complex thermo-physical and chemical process with homogeneous gas reactions and heterogeneous reactions ocurring on the porous matrix of the wood. This paper describes a simplified numerical model of the burning of wood cylinders under a constant heat flux, including the simultaneous vaporization, pyrolysis and smoldering phases. Numerical results obtained for Pinus elliot wood are compared to experimental data.*

Keywords. Combustion, wood, pyrolysis, cylinder, drying, numerical model.

1. Introduction

The capability to predict the burning rate of wood in modern times has become increasingly important as fire safety engineering moves toward a performance-based approach to building design (Spearpoint, 1999, 2001).

Combustion of biomass, mainly wood, releases pollutants in the atmosphere, increasing global warming, acid rain formation, production of smoke and particulates. It causes direct problems to the health of populations, worsen visibility conditions, produces ecological unbalance with reduction in biodiversity, damage the biogeochemical cycles and other adverse effects (Crutzen e Andreae, 1990). It should be noted that biomass combustion in furnaces, burners or rotary kilns can have less hazardous consequences, if control of emissions is implemented.

Burning of wood presents several phases: pre-heating, drying, ignition, pyrolysis, flaming, flame extinction, smoldering and smoldering extinction. The flaming phase occurs when the volatiles from wood pyrolysis mix with air above the lean flammability limit in the boundary layer adjacent to the wood sample, and the gas temperature is above the ignition point (Kanury, 1977). Smoldering is a slow flameless heterogeneous burning process in which the residual char from pyrolysis is oxidized by air. Smoldering can last several days after fires, especially in the case of large logs or ground vegetation. Several of these phases can occur simultaneously, for example, drying and pyrolysis.

The role played by moisture transport phenomena is dependent on the heating conditions. In relatively low temperatures free water capillarity and diffusion of bound water play a controlling role, with liquid-phase flows two or three orders of magnitude larger than the vapor fluxes. The high-temperature behavior has been simulated by Di Blasi et al. (2003) by considering the propagation of an evaporation front during the entire duration of the process together with significant gas phase convective transport. In general, the presence of moisture introduces a delay in the heating time, with consequent variations in reaction temperatures, product distribution and ignition times.

The effects of moisture on burning characteristics of tropical woods have been studied experimentally by Castro (2005) and Castro and Costa (2005). An analysis of the effects of sample diameter and heat input on combustion characteristics of *Pinus elliot*, a common softwood in Brazil, using a cylindrical calorimeter was also made by Castro and Costa (2005). A theoretical model of burning of wood cylinders was presented by Costa et al. (2003).

Several numerical models of the wood burning have been developed, mostly focusing on a single phase of the whole process. Tinney (1965) compared numerical results of a thermal model with experimental results of burning cylinders of wood under heated air. Roberts (1970) made a review of the influence of the kinetics on pyrolyis of wood and cellulosic materials. Kanury (1972) analysed the carbonization rate of wood, adopting an Arrhenius kinetics for the pyrolysis process. Tzeng e Atreya (1991) developed a detailed model of finite differences for the ignition process to compare to their experimental observations. Quintiere (1992) developed an integral one-dimensional model of pyrolysis. Saastamonien and Richard (1996) presented detailed numerical simulations of the simultaneous drying and pyrolysis of biomass. Spearpoint (1999) compared ignition and burning rate data obtained in a conical calorimeter with an integral one-dimensional model describing the transient pyrolysis of a charring semi-infinite solid under a constant heat flux. Bilbao et al. (2001) presented theoretical and experimental studies of wood ignition, including convection effects; the experimental study included tests with self-ignition and piloted ignition, both with different air flow rates on the samples. Di Blasi et al. (2003) investigated experimentally the drying of Pinus cylinders in a fixed bed under a counter-current of heated air (air coming from the top); a simplified numerical model of the drying process of the samples was proposed and presented good agreement with the experimental data.

There is still a limited amount of data in literature related to the drying, pyrolysis and burning processes of tropical woods under controlled conditions. Therefore, the objective of this work is to present a simplified numerical model to describe the combustion process of *Pinus elliot* wood cylinders including all phases of burning and to compare the numerical results with experimental data.

2. Model Description

The present numerical model extends the wood drying model developed by Di Blasi et al. (2003) to include the simultaneous pyrolysis and smoldering processes. Figure 1 shows a schematic view of the complete process of drying and burning of a wood cylinder under a constant heat flux.

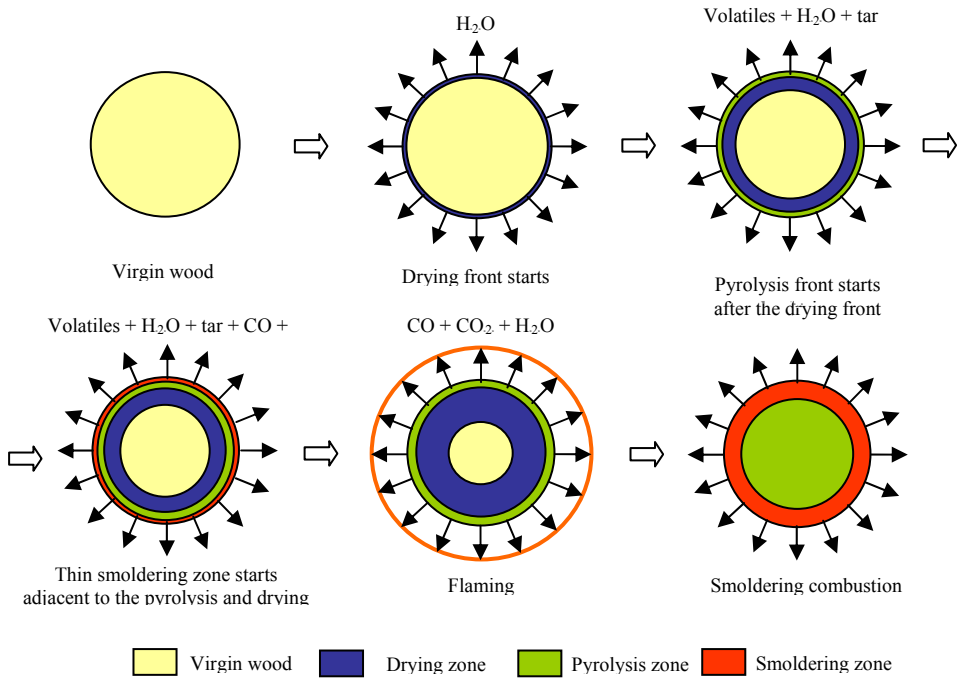

Figure 1 – Phases of drying and burning of a wood cylinder under a constant external heat flux.

It is assumed that wood has four main components: ash, water, pyrolysate and char. Thus, it follows that

$$\rho_f = \rho_a + \rho_c + \rho_l + \rho_p \tag{1}$$

where ρ_i is the apparent density of phase i and the subscripts f, a, c, l and p denote, respectively, wood, ash, char, water and pyrolysate.

Figure 2 shows a cylindrical ring of thickness dr inside a wood cylinder of radius a, located at a distance r of the center. Note that ρ_i is the ratio between the mass of component i inside the cylindrical ring and its volume, and therefore, it does not represent the real density of the phase, but its apparent density.

2.1. Mass Balances

A balance of the mass of water inside the cylindrical ring of thickness dr gives:

$$\frac{\partial \rho_l}{\partial t} + \frac{1}{r}\frac{\partial \left(r \dot{m}_l''\right)}{\partial r} = \dot{m}_l''' \tag{2}$$

where the first term on the left side represents the time variation of liquid water inside the volume element, the second term represents the flow of water across the cylindrical ring and the term on right is the vaporization rate of water inside the element of volume.

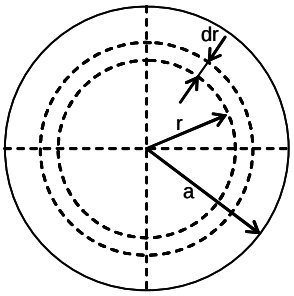

Figure 2 – Cylindrical ring of thickness *dr*.

Assuming that there is no liquid flow inside the pores, $\dot{m}_l'' = 0$, then:

$$\frac{\partial \rho_l}{\partial t} = \dot{m}_l''' \tag{3}$$

The balance of water vapor inside the volume element yields

$$\frac{\partial \rho_w}{\partial t} + \frac{1}{r}\frac{\partial (r\dot{m}_w'')}{\partial r} = \dot{m}_w''' \tag{4}$$

where $\dot{m}_w'''$ is the rate of formation (> 0) of water vapor inside the volume element and $\dot{m}_w''$ is the radial flow of vapor across the cylindrical ring. Once

$$\dot{m}_l''' = -\dot{m}_w''' \tag{5}$$

then

$$\frac{\partial \rho_w}{\partial t} + \frac{1}{r}\frac{\partial (r\dot{m}_w'')}{\partial r} = -\frac{\partial \rho_l}{\partial t} \tag{6}$$

Assuming that $|\partial \rho_w / \partial t| << |\partial \rho_l / \partial t|$, since the gas density is much lower than the apparent density of water (different from the real density of water), it follows that:

$$\frac{\partial \rho_l}{\partial t} + \frac{1}{r}\frac{\partial (r\dot{m}_w'')}{\partial r} \cong 0 \tag{7}$$

Similarly, for the pyrolisate, it results:

$$\frac{\partial \rho_p}{\partial t} + \frac{1}{r}\frac{\partial (r\dot{m}_v'')}{\partial r} \cong 0 \tag{8}$$

Assuming that only *CO* and CO_2 (= CO_x) are produced by the char, it follows that $\dot{m}_c''' = -s\dot{m}_{COx}'''$, where *s* is a stoichiometric "mass" coefficient. For $C + O_2 \rightarrow CO_2$, s = 12/44 = 3/11 and for $C + O \rightarrow CO$, *s* = 12/28 = 3/7. Therefore, it can be written for the char oxidation:

$$\frac{\partial \rho_c}{\partial t} + \frac{s}{r}\frac{\partial (r\dot{m}_{COx}'')}{\partial r} \cong 0 \tag{9}$$

2.2. Energy Balance

An energy balance along the cylindrical ring of thickness *dr* yields:

$$\left(\rho_a c_a + \rho_l c_l + \rho_p c_p + \rho_c c_c\right)\frac{\partial T}{\partial t} = \frac{1}{r}\frac{\partial}{\partial r}\left(r\lambda \frac{\partial T}{\partial r}\right) - \left(c_v \dot{m}_v'' + c_w \dot{m}_w'' + c_c \dot{m}_{COx}''\right)\frac{1}{r}\frac{\partial (rT)}{\partial r} - L_l \frac{\partial \rho_l}{\partial t} - L_p \frac{\partial \rho_p}{\partial t} - L_c \frac{\partial \rho_c}{\partial t} \tag{10}$$

In Equation (10) the term on the left side represents the variation of internal energy inside the element volume, the first term on the right side represents heat conduction, the second represents the convective flow of energy, the third represents a heat sink for water vaporization, the fourth represents a heat source or sink for pyrolysis of wood, the fifth term represents a heat source for char oxidation. It is assumed that gases and solid are in thermal equilibrium. The variable T is the temperature; λ is the thermal conductivity of the wood; c_i, $i = a, l, p, c,$ are the specific heats of ash, liquid water, pyrolysate and char, respectively; L_i, $i = w, v, CO_x$, are the heat of vaporization, pyrolysis and of char oxidation, respectively.

2.3. Reaction Rates

The rates of drying, pyrolysis and char oxidation can be described by Arrhrenius kinetics:

$$\frac{\partial \rho_l}{\partial t} = -k_l \rho_l \qquad \text{where} \qquad k_l = A_l \exp\left(-T_{a,l}/T\right) \tag{11}$$

$$\frac{\partial \rho_p}{\partial t} = -k_p \rho_p \qquad \text{where} \qquad k_p = A_p \exp\left(-T_{a,p}/T\right) \tag{12}$$

$$\frac{\partial \rho_c}{\partial t} = -k_c \rho_c Y_{O2} \qquad \text{where} \qquad k_c = A_c \exp\left(-T_{a,c}/T\right) \tag{13}$$

The activation temperatures are given by $T_{a,i} = E_{a,i} / R_0$, where $E_{a,i}$ is the activation energy of reaction i and R_0 is the universal gas constant.

3. Boundary Conditions and Thermal Properties

The boundary conditions for the problem are:

$$\frac{\partial T}{\partial r} = \dot{m}''_v = \dot{m}''_w = \dot{m}''_{COx} = 0 \qquad \text{at} \quad r = 0 \tag{14}$$

$$\lambda \frac{\partial T}{\partial r} = h_c\left(T_a - T\right) + \dot{q}''_h \qquad \text{at} \quad r = a \ \text{(no flame)} \tag{15}$$

or

$$\lambda \frac{\partial T}{\partial r} = h_c\left(T_a - T\right) + \dot{q}''_h + \varepsilon\sigma\left(T_f^4 - T^4\right) \qquad \text{at} \quad r = R \ \text{(flaming)} \tag{16}$$

where $\dot{q}''_h$ is the radiation heat input from the heater, or neighborhood, and T_f is the flame temperature.

The eflux of volatiles, CO, CO_2 and water vapor reduce the convection heat transfer along the cylinder wall, h_c, according to:

$$\frac{h_c}{h_{c,o}} = \frac{B}{e^B - 1} \tag{17}$$

with

$$B = \frac{c_v \dot{m}''_v + c_w \dot{m}''_w + c_c \dot{m}''_{COx}}{h_{c,o}}, \tag{18}$$

where B is the blowing factor, similar to a simpler one used by Di Blasi et al. (2003). The fractions of liquid water X_l, pyrolysate X_p and char X_c inside a volume element are given by:

$$X_l = \rho_l / \rho_f \qquad ; \qquad X_p = \rho_p / \rho_f \qquad ; \qquad X_c = \rho_c / \rho_f \tag{19a,b,c}$$

The thermal conductivity λ and the specific heats c_i, $i = l,p,c$, vary with temperature and are calculated by the approximate expressions:

$$\lambda = \lambda_0 \frac{\rho_f}{\rho_{f,0}} \left(\frac{T}{T_0} \right)^{0,5} , \quad i = l, p, c \tag{20}$$

$$c_i = c_{i0} \left(\frac{T}{T_0} \right)^{0,5} , \quad i = l, p, c \tag{21}$$

4. Simplified Energy Equation

The equation for the balance of energy can be written as:

$$\rho c \frac{\partial T}{\partial t} = \frac{1}{r} \frac{\partial}{\partial r} \left(r \lambda \frac{\partial T}{\partial r} \right) - c_g \left(\dot{m}_v'' + \dot{m}_w'' + \dot{m}_{COx}'' \right) \frac{1}{r} \frac{\partial (rT)}{\partial r} - L_l \frac{\partial \rho_l}{\partial t} - L_p \frac{\partial \rho_p}{\partial t} - L_c \frac{\partial \rho_c}{\partial t} \tag{22}$$

where $\rho c = \rho_a c_a + \rho_c c_c + \rho_l c_l + \rho_p c_p$ is the total heat capacity of wood and $c_g = c_w = c_v = c_{COx}$ is the specific heat of the gas phase, which is taken as a constant average value.

The boundary conditions are rewritten as:

$$\frac{\partial T}{\partial r} = \frac{\partial \rho_f}{\partial r} = \frac{\partial \rho_l}{\partial r} = \frac{\partial \rho_p}{\partial r} = \frac{\partial \rho_c}{\partial r} = 0 \quad \text{em} \quad r = 0 \tag{23}$$

$$\lambda \frac{dT}{dr} = h(T_\infty - T) \quad \text{em} \quad r = R \tag{24}$$

where h is an effective heat transfer coefficient including convection and radiation and T_∞ is the ambient temperature, flame temperature or the freestream flow temperatures around the cylinder.

The process of char oxidation can be controlled by the oxygen diffusion or by heterogenous reaction rate inside the porous matrix, which depends on temperatures, pressure and char composition. Oxygen diffusion depends on geometry and pore distribution, volatiles and water vapor convection, temperature and pressure. As a first approximation, a linear profile of oxygen inside the pyrolysed region was adopted:

$$Y_{O2} \cong \left(1 - \frac{\rho_p}{\rho_{p,0}} \right) Y_{O2,\infty} \tag{25}$$

where $Y_{O2,\infty}$ is the mass fraction of oxygen in the ambient.

It is assumed that ignition occurs when the mixture F/O between volatiles and air attains the lean flamability limit inside the boundary layer at the ignition temperature. At end of pyrolysis the mixture ratio F/O decreases with the exhaustion of volatiles and flame extinction occurs.

During flaming it is assumed that there is no penetration of oxygen inside the flame and there is no char oxydation.

5. Numerical Solution and Results

The simplified equations (22)-(24), with the auxiliary equations, were discretized by an explicit finite difference scheme. A Matlab 6.5 code was written and time steps of 0.02 s with 13 radial points were adopted, for simulation of the burning process of a *Pinus elliot* wood cylinder with 30 mm diameter. The input data required for the simulations are listed on Table 1. Several runs of the code with different timesteps were made until convergence was achieved.

Figures 3, 4 and 5 show, respectively, the mass evolution, mass consumption rate and normalized mass consumption rates of cylinders with 20 and 40 % of moisture content, on dry basis. Numerical results and experimental data are presented. The evolution of the total mass, water mass and the pyrolysate mass are shown. Ignition was assumed to occur for mass flow rates of volatiles higher than 0.06 g/s.

Experiments were performed inside a cylindrical calorimeter with wood cylindrical samples burned under a heater input of 2000 W. Several samples with given moisture content were burned. The experimental setup, sample preparation and the test sequence are described in detail by Castro (2005).

The simulation shows that pinus cylinders with 20 % moisture content presented simultaneous drying and flaming while cylinders with 40 % moisture content presented simultaneous drying and pyrolysis, for the same heat input. Cylinders with higher moisture contents require larger heat power input to vaporize the water and, therefore have lower propensity to ignite.

Table 1 - Input data for the simulations of *Pinus elliot* cylinders.

data	variable	value
Initial total mass of cylinder	$m_{o,0}$	0.026 kg
Initial char mass of cylinder	$m_{c,0}$	0.181$m_{o,0}$ kg
Initial dry wood apparent density	$d_{d,0}$	368 kg/m^3
Initial char apparent density	$d_{c,0}$	67 kg/m^3
Initial pyrolysate apparent density	$d_{p,0}$	301 kg/m^3
Cylinder radius	r_o	0.015 m
Freestream temperature	T_f	800 K
Initial temperature	T_o	300 K
Pre-exponential factor of water vaporization	A_l	6.7E3 1/s
Pre-exponential factor of pyrolysis	A_p	6.0E3 1/s
Pre-exponential factor of char oxidation	A_c	7.5E1 1/s
Activation temperature of water vaporization	$T_{a,l}$	5500 K
Activation temperature of pyrolysis	$T_{a,p}$	7000 K
Activation temperature of char oxidation	$T_{a,c}$	10500 K
Effective convection coefficient	h	100 W/m^2/K
Heat of water vaporization	L_l	2.245E6 J/kg
Heat of pyrolysis	L_p	0.300E6 J/kg
Heat of char oxidation	L_c	20.000E6 J/kg
Initial thermal conductivity	$\lambda_{f,0}$	0.14 W/mK
Specific heat of pyrolysates	c_p	1500 J/kg/K
Specific heat of char	c_c	670 J/kg/K
Specific heat of liquid water	c_l	4170 J/kg/K
Specific heat of gas phase	c_g	1500 J/kg/K

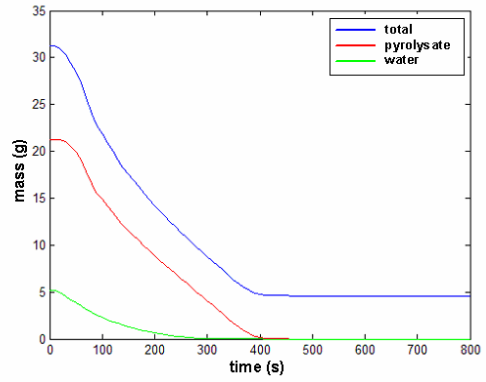

a) 20% H2O – Numerical

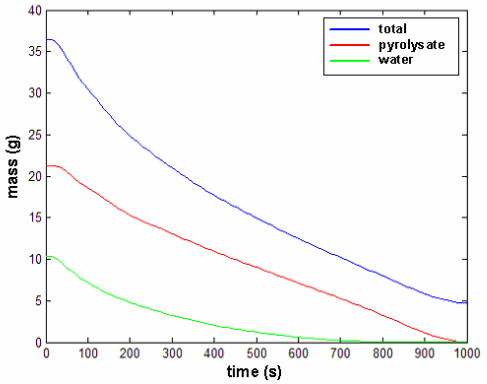

b) 40 % – Numerical

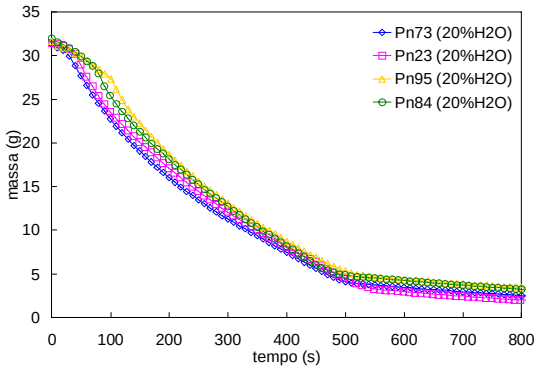

c) 20% H2O – Experimental

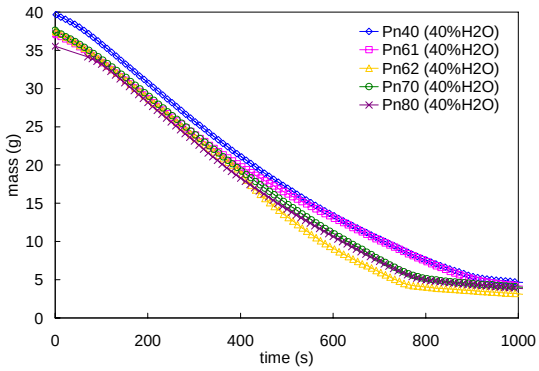

d) 40 % H2O – Experimental

Figure 3 – Mass evolution of pinus cylinders.

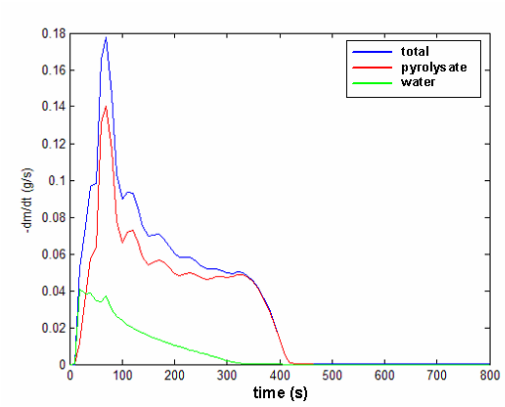

a) 20% H2O – Numerical

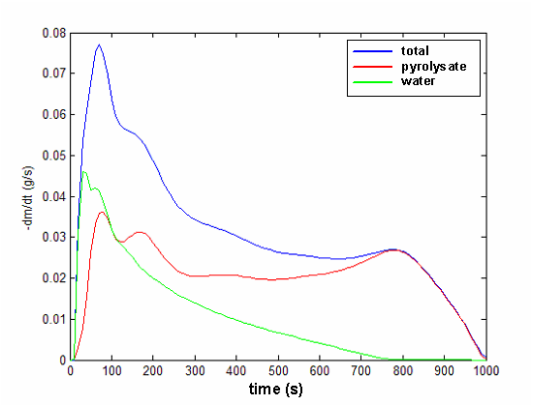

b) 40 % – Numerical

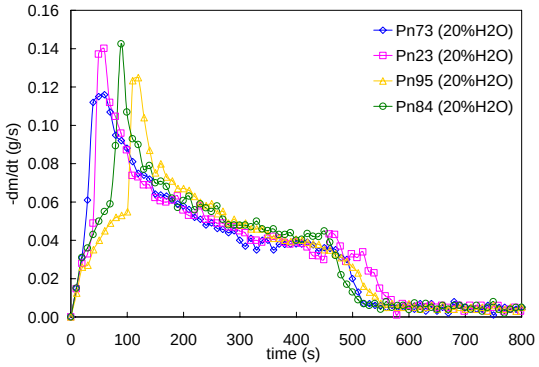

c) 20% H2O – Experimental

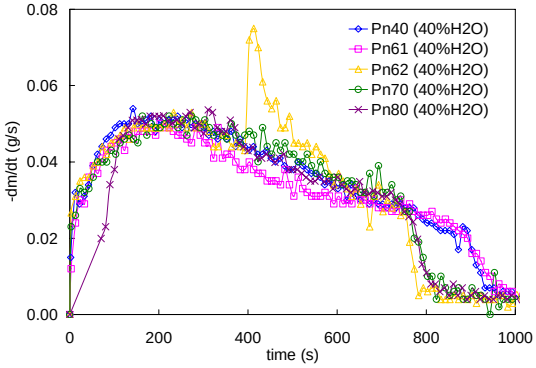

d) 40 % H2O – Experimental

Figure 4 – Mass consumption rates of pinus cylinders.

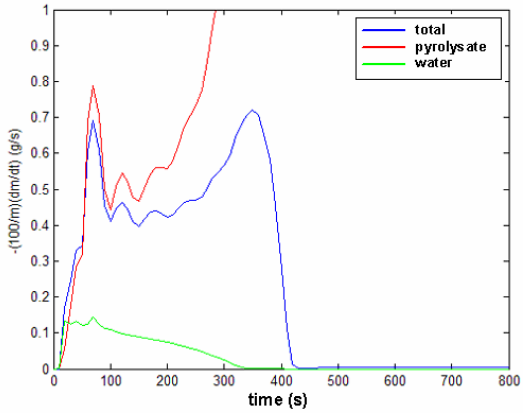

a) 20% H2O – Numerical

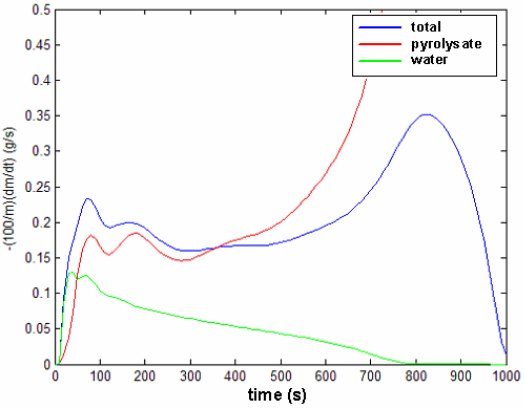

b) 40 % – Numerical

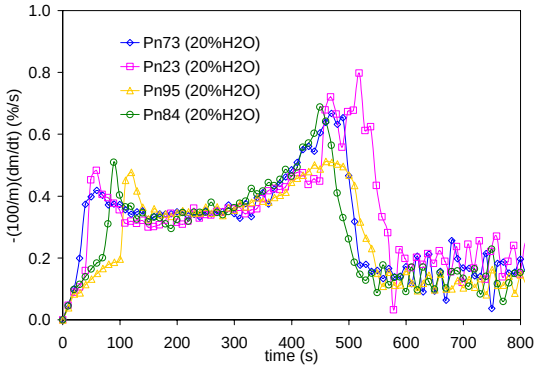

c) 20% H2O – Experimental

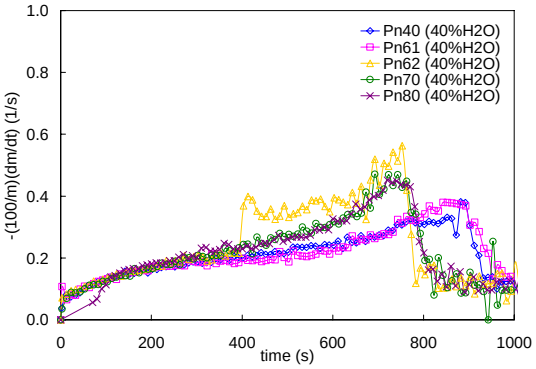

d) 40 % H2O – Experimental

Figure 5 – Normalized mass consumption rates of pinus cylinders.

The numerical smoldering rates were very lower than the experimental ones. Further studies are required to better simulate the smoldering phase, for example, modifying the oxygen profiles inside the cylinder. More detailed simulations are being implemented to compare different wood species and water contents, including property variations.

6. Conclusions and Comments

This work describes a simplified numerical model to simulate the burning behavior of wood cylinders. The numerical results are compared to the numerical simulations, showing a good agreement, despite the simplifying assumptions. It was assumed that vaporization, pyrolysis and smoldering processes follow the Arrhrenius kinetics. However, it is well-known that pyrolysis can be better described by a two step process: an endothermic one followed by an exothermic one, resulting in a global reaction with almost zero heat of reaction. Flow of liquid water inside the wood was not considered.

8. Acknowledgement

The authors acknowledge FAPESP for supporting this research.

9. References

Bilbao, R.; Mastral, J. F.; Aldea, M. E.; Ceamanos, J. Experimental and theoretical study of the ignition and smoldering of wood including conve ctive effects. *Combustion and Flame*, v. 126, n. 1-2, p. 1363-1372, 2001.

Castro, A, Uma Investigação Teórico-Experimental da Combustão de Madeira, *Master Thesis*, INPE, SP, Brazil, 2005.

Castro, A., Costa, F.S., Effects of Moisture Content on Burn Rates and Characteristic Times of Brazilian Woods, *18th International Congress of Mechanical Engineering*, Ouro Preto, MG, Brazil, 2005.

Castro, A., Costa, F.S., Effects of Diameter and Heat Flux on Burning Characteristics of Wood Cylinders, *18th International Congress of Mechanical Engineering*, Ouro Preto, MG, Brazil, 2005.

Castro, A., Costa, F.S., Numerical Simulation of the Burning of Wood Cylinders, *18th International Congress of Mechanical Engineering*, Ouro Preto, MG, Brazil, 2005.

Crutzen, P.J., Andreae, M.O., Biomass Burning in the Tropics: Impact on Atmospheric Chemistry and Biogeochemical Cycles, *Science*, 250, 1669, 1990.

Costa, F.S., Castro, A., Carvalho-Jr. J.A., Burning Characteristics of Wood Cylinders, *17th International Congress of Mechanical Engineering*, São Paulo, SP, Brazil, 2003.

Di Blasi, C., Branca, C., Sparano, S., La Mantia, B., Drying characteristics of wood cylinders for conditions pertinent to fixed-bed countercurrent gasification, *Biomass and Bioenergy*, v. 25, n. 1, p. 45-58, 2003.

Kanury, A.M., Ignition of Cellulosic Solids: Minimum Pyrolysate Mass Flux Criterion, *Combustion Science and Technology*, Vol. 16, p.89, 1977.

Kanury, A. M. Rate burning of wood: a simple thermal model. Combustion Science and Technology, v. 5, n. 4, p. 135-146, 1972.

Galgano, A., Di Blasi, C., Modeling the Propagation of Drying and Decomposition Fronts in Wood, *Combustion and Flame*, Vol. 139: 16–27, 2004.

Quintiere, J.G., A semi-quantitative model for the burning rate of solid materials, *Report NISTIR 4840*, 42p. Gaithersburg, MD, 1992.

Roberts, A. F. Review of kinetics data for pyrolysis of wood and related substances, *Combustion and Flame*, v. 14, n. 1-3, p. 261–272, 1970.

Saastamoinen, J., Richard, J.R., Simultaneous Drying and Pyrolysis of Solid Fuel Particles, *Combustion and Flame*, Vol. 106: 288-300, 1996.

Spearpoint, M.J., Predicting the Ignition and Burning Rate of Wood in the Cone Calorimeter using an Integral Model, Building and Fire Research Laboratory, *Report NIST GCR 99-775*, Maryland, USA,1999.

Spearpoint, M.J., Quintiere, J.G., Predicting the Burning of Wood using an Integral Model, *Combustion and Flame*, 123:308-324, 2001.

Tinney, E. R. The combustion of wooden dowels in heated air. In: International Symposium on Combustion, 10, 17-21 Aug. 1964, Cambridge. *Proceedings…,* Pittsburgh, PA: The Combustion Institute p. 925-930, 1965.

Tseng, L., Atreya, A., Theoretical investigation of piloted ignition of wood, *Report NIST-GCR-91-595*, Gaithersburg, MD, 1991.